JOURNAL OF GEOPHYSICAL RESEARCH, VOL. 106, NO. A11, PAGES 24,813–24,829, NOVEMBER 1, 2001

Retrieval and validation of mesospheric temperatures from Wind Imaging Interferometer observations

Marianna G. Shepherd, Boedijanti Reid,[1] Shengpan Zhang,[2] Brian H. Solheim, and Gordon G. Shepherd

Centre for Research in Earth and Space Science, York University, Toronto, Canada

Vincent B. Wickwar and Joshua P. Herron

Center for Atmospheric and Space Sciences, Utah State University, Logan, Utah

Abstract. A method has been developed for the retrieval of mesospheric temperatures in the 65-90 km altitude range from satellite observations made by the Wind Imaging Interferometer (WINDII) aboard the Upper Atmosphere Research Satellite (UARS). Retrieved temperatures are derived from Rayleigh scattered sunlight observed in a wavelength band centered at 553 nm. Integrated line-of-sight radiance observations are inverted to tangent height volume scattering profiles, which are proportional to atmospheric density. From these, absolute temperature profiles are calculated using a technique derived from established Rayleigh lidar retrieval methods assuming that the atmosphere is in hydrostatic equilibrium and that it obeys the ideal gas law. Sources of error have been identified and typical temperature uncertainty values for individual profiles are determined to be < 2.5%, 5.5%, and 13% for altitudes of 70 km, 80 km, and 90 km, respectively. A thorough comparison of the derived WINDII temperatures is performed against a number of ground-based and satellite measurements, including ground-based lidar, falling spheres, the High Resolution Doppler Imager observations aboard UARS, and against common atmospheric models. The data consist of spring equinox observations in March and April 1992/1993, summer solstice data in July/August 1992/1993, fall equinox data in September/October 1992, and winter solstice data in December 1992/1993 and January 1993/1994. The results of the comparisons show that WINDII temperatures are in reasonable to excellent agreement with a number of established temperature studies. In particular, July Northern Hemisphere monthly averaged temperatures show that characteristics of the mesopause obtained by WINDII are in very good agreement with other measurements. This good agreement with other established data sets and a determination of the error bounds of our recovered temperatures have shown that WINDII data can be used to confidently derive near-global temperatures of the upper mesosphere between 65 and 90 km. Above 90 km the errors increase, and systematic differences may arise with other measurements.

1. Introduction

Understanding the thermal structure of the mesosphere/lower thermosphere region has been gained through a variety of in situ and remote sensing temperature observations. The dominant source of temperature information comes from ground-based lidar [i.e., *Hauchecorne et al.*, 1991; *She et al.*, 1993; *Yu and She*, 1995; *Chen et al.*, 2000; *States and Gardner*, 2000a, 2000b], airglow observations [*Wiens et al.*, 1991], in situ rocket-based measurements [i.e., *Lübken and von Zahn*, 1991; *Lübken et al.*, 1996; *Lübken*, 1999] and in the last decade, from satellite missions like the SME [*Clancy and Rusch*, 1989; *Clancy et al.*, 1994] and UARS [*Reber et al.*, 1993]. While lidar and falling sphere observations provide vertical temperature profiles with several hundreds of meters resolution, they are restricted to only a given site, predominantly in the Northern Hemisphere. Satellite-based observations have poorer resolution, typically 2-4 km, but have the distinct advantage of providing routine global coverage which cannot be achieved by ground-based or rocket observations.

One of the first global temperature climatologies was produced from satellite observations made by the Solar Mesosphere Explorer (SME) [*Clancy and Rusch*, 1989]. More recent middle atmosphere temperatures have been acquired by the Improved Stratospheric and Mesospheric Sounder (ISAMS) [*Dudhia and Livesey*, 1996; *Taylor et al.*, 1993], the High-Resolution Doppler Imager (HRDI) [*Ortland et al.*, 1998], the Microwave Limb Sounder (MLS) [*Fishbein et al.*, 1996] and the Wind Imaging Interferometer (WINDII) [*Evans et al.*, 1994; *Shepherd et al.*, 1997], all aboard the Upper Atmosphere Research Satellite (UARS) launched in September 1991.

Experimental data from lidars and satellites are often compared to atmospheric models such as the COSPAR (Committee on Space Research) International Reference Atmosphere

[1]Now at 4DM Inc., Toronto, Ontario, Canada.
[2]Now at MIT Haystack Observatory, Westford, Massachusetts.

Paper number 2000JA000323.
0148-0227/01/2000JA000323$09.00

(CIRA-86) [*Fleming et al.*, 1988] and Mass Spectrometer Incoherent Scatter (MSIS-90) [*Hedin*, 1991], although good comparative results are not always achieved. Potential reasons for discrepancies between models and more current experimental data may be attributed to the older data sets used to create the models. Below 80 km CIRA-86 uses satellite data collected by the Selective Chopper Radiometer (SCR) between 1973 and 1974 and the Pressure Modulator Radiometer (PMR) between 1975 and 1978. Above 86 km, the model uses MSIS-83 and MSIS-86 values gathered by instruments such as rocket borne and satellite mass spectrometers, falling spheres, and incoherent scatter radar. MSISe-90 is a revised version of CIRA-86, which attempts to more successfully merge the top of the SCR/PMR data to the bottom of the MSIS-83/MSIS-86 models. Often the edges of data sets are the most erroneous, and some attempts to link the two models resulted in interpolated temperatures not obeying standard atmospheric relationships and not in agreement with experimental data. It is clear that more current and continuous data sets are needed to more accurately characterize this region of the atmosphere. To provide information to help update global atmospheric models is just one of the motivations to measure temperatures of the upper mesosphere.

Temperature sounding of the mesosphere is also needed to further study some of the poorly understood processes within this region. Two interesting features observed in this region are mesospheric temperature inversions [*Leblanc and Hauchecorne*, 1997; *Meriwether et al.*, 1998] in the height range of 75-80 km at low and middle latitudes and mesospheric clouds (MC) (also called noctilucent, NLC, and polar mesospheric clouds, PMC) [*Thomas*, 1991]. The latter are observed during the summer at high latitudes below the mesopause at ~82 km [*Lübken et al.*, 1996]. Temperature measurements in the polar regions will help to explain the conditions surrounding the formation and occurrence of this phenomenon.

The dynamics of the upper mesosphere and mesopause region are not well understood. Certain measurement techniques employed by satellite instruments can allow for daytime measurements which complement the growing number of lidar data taken mostly at night. This will allow for a complete diurnal study of upper atmospheric temperatures and may provide more evidence for the existence of mesospheric inversion events in the daytime as well as in the night. In this regard, the experimental data acquired during the UARS mission are well suited to facilitate the study of the middle atmosphere, including the upper mesosphere and lower thermosphere (MLT) region in particular.

2. WINDII Temperature Observations

Upper mesospheric temperatures are derived using radiance measurements by the background filter for the atomic oxygen green line. This filter (filter 1) is centered at 553.1 nm wavelength with a bandwidth of 1.6 nm, responding in daytime to the spectrum of the Rayleigh scattered solar continuum. The WINDII measurements are taken at the Earth's limb. For this viewing geometry, radiation is observed tangentially through the atmospheric layers. The main advantage of limb viewing is that the measured data are heavily weighted around the tangent height which is the lowest altitude probed along the line of sight (LOS). As the radiance and thus the atmospheric density decrease exponentially with height, the weighting functions peak sharply at the tangent points, implying that most of the information comes from the region adjacent to these tangent points.

The data analyzed in this work employ WINDII's field of view 1 (FOV 1). The vertical resolution (bin) of the data is 2.2 km, and the horizontal resolution (bin) is 25 km. Each image has ~26 vertical bins and 6 horizontal bins with the tangent heights typically ranging between 65 and 115 km. Orbital constraints and instrument viewing geometry allow WINDII to observe maximum latitudinal coverage from 42° in one hemisphere to 72° in the other. The UARS orbit processes at rate of ~5°d^{-1} as a result of an orbital inclination of 57°. This orbital configuration, coupled with WINDII's viewing geometry, requires 36 days to provide full daytime local time coverage. Equivalently, observed points along a latitude circle are seen to change in local time by ~20 min for each consecutive day. Depending on the WINDII observation schedule, the sampling of the atmosphere by the background filter may not cover the entire month uniformly in local time. The WINDII measurements used are labeled as "level 1" data where the signal in digital units has been converted to Rayleighs using the responsivity of each bin after the dark current signal has been subtracted. A detailed description of the WINDII instrument and measurements is provided by *Shepherd et al.* [1993].

The WINDII Rayleigh-scattering temperatures are not part of the WINDII data product and thus required off-line processing. Some early results were reported by *Shepherd et al.* [1997] and *Evans et al.* [1994], where the retrieval procedure first involved calculating the scale height by fitting the observed integrated radiance at each altitude, from which by applying hydrostatic equilibrium and the ideal gas law the apparent temperature at that height was derived. The final temperatures were then recovered by applying an inversion method directly to the apparent temperatures [*Shepherd et al.*, 1997].

3. The WINDII Temperature Retrieval

The current temperature retrieval algorithm consists of two steps. First, Chahine's relaxation method is applied to the integrated line of sight radiance data to retrieve tangent height volume-scattering rate profiles which are a relative measure of atmospheric density. Further, temperatures from the density-height profiles are calculated using the hydrostatic equation and the ideal gas law. The latter step of deriving temperatures from densities is patterned after the method used to derive Rayleigh lidar temperatures. In the past, a similar method was employed to retrieve densities and temperatures from the SME satellite observations [*Clancy and Rusch*, 1989].

Chahine's relaxation method for the inverse solution to linear and nonlinear radiative transfer equations can be used to derive atmospheric functions, such as temperature and composition profiles, from radiance data [*Chahine* 1970, 1972, 1977]. The method can specifically be employed in cases where the weighting functions have well-defined peaks and thus is well suited for the WINDII inversion problem.

In brief, the measured radiance at given altitude is expressed as a solution of a set of integral equations of the volume-scattering rates (VSR) along the line of sight (LOS). For the linear case, the solution of these integral equations comes from finding values of VSR, which when substituted into the equations, yield radiance values such that in the final solution they are equal to the corresponding measured radiances within

acceptable differences. Using an initial guess for VSR for all altitudes in the 65-90 km range, Chahine's method is applied as follows.

The relaxation equation is derived as [*Chahine,* 1970, 1972]:

$$\frac{q^{(n+1)}(z)}{q^{(n)}(z)} \approx \frac{\tilde{I}(z_0)}{I^{(n)}(z_0)}, \tag{1}$$

where $q^n(z)$ is the nth guess of the VSR, $q(z)$, of the iterative solution, $q^{(n+1)}(z)$ is the $(n+1)$th guess of the solution, and $I^{(n)}(z_0)$ at the tangent height z_0 is computed from $q^n(z)$. Then at each altitude a residual $r^{(n)}(z)$ is calculated as the ratio of the difference between the measured WINDII radiances $\tilde{I}$ and the solution $I^{(n)}(z)$, on one hand and the $\tilde{I}$, on the other. The $q^n(z)$ is the solution if all of the residuals $r^{(n)}(z)$ approach zero; otherwise from (1) a new guess for $q^{(n+1)}(z)$ is obtained at all altitudes and the process is repeated until a suitable set of $q(z)$ is found.

To obtain the VSR from the measured LOS radiances, we need to specify the path lengths along each LOS corresponding to a given tangent height for the WINDII limb viewing geometry. Using the assumption that the atmosphere is composed of a discrete number of spherical layers that are horizontally uniform and applying simple geometrical considerations, the path length (in kilometers) along a particular LOS is determined in a fashion similar to that described by *Rogers* [1976] and *Rochon* [1999].

The iterative method is terminated if three criteria are met. First, it terminates if the residuals $r^n(z)$ are sufficiently small. While it is desirable for the residuals $r^n(z)$ to be small, indicating that the retrieved function corresponds to the true value, it is impossible to presume the existence of a set of $q(z)$ such that Equation (1) be completely satisfied. *Chahine* [1977] has shown that, in general, the iteration can be terminated when the residuals reach a relatively constant value of the same order of magnitude as the errors in the original measurements. For the WINDII Rayleigh-scattering radiances the signal-to-noise ratio (SNR) decreases with height as does the atmospheric density, and on average above 90 km the retrieved temperatures become very noisy. In the current version of the temperature algorithm the retrieval process stops if the average root- mean-square (RMS) deviation of the residual over all heights becomes < 0.1% at and below 90 km. The process is also terminated if the average percentage difference between two consecutive relative densities is < 0.25% at a given latitude below 90 km for three consecutive iterations. The final stopping criterion deals with the maximum number of iterations the retrieval routine can perform; this is set to 30 iterations. If the retrieved value does not converge within these 30 iterations, the profile is rejected.

The retrieval of temperatures from densities is similar to that of Rayleigh lidar studies [e.g., *Chanin and Hauchecorne,* 1984; *Whiteway,* 1994]. Assuming that scattering by aerosols is negligible above 30 km [*Hauchecorne et al.,* 1991], in both the Rayleigh lidar and WINDII cases, the measured backscattered signal is proportional to atmospheric density. Starting from an estimated value of pressure from the CIRA-86 model atmosphere [*Fleming et al.,* 1988] at the top of the relative density profile, the hydrostatic equation is integrated downward using the observed densities to determine the relative pressure at the top and bottom of each bin Δz. The absolute temperature is derived from the pressure at the bottom and top of each altitude interval as [e.g., *Hauchecorne et al.,* 1991]

$$T(z) = \frac{m(z)g(z)\Delta z}{k\left[\ln\frac{p(z-(\Delta z)/2)}{p(z+(\Delta z)/2)}\right]}. \tag{2}$$

The correctness of the WINDII retrieval algorithm was tested by simulating lidar-measured radiances using a typical inverted radiance profile from WINDII in the height range 65-120 km. From these pseudo-lidar radiances a temperature profile was obtained after employing a lidar temperature-retrieval algorithm [i.e., *Chanin and Hauchecorne,* 1984; *Whiteway,* 1994] with a reference pressure point at 114 km height derived from the MSIS model. The "lidar" temperature profile obtained was compared with that retrieved by the WINDII algorithm using the same inverted VSR. The WINDII/"lidar" temperature difference was 1.6 K below 90 km with the WINDII temperatures being the warmer of the two. The test confirmed that the WINDII retrieval method is able to effectively invert LOS radiances to tangent height radiances/densities from which meaningful temperatures are obtained using a lidar-type algorithm.

As mentioned earlier, each raw image consists of six adjacent columns of radiances each with a horizontal resolution of 25 km. On occasion, some of these column radiances are contaminated by non-Rayleigh-type scattering, and temperatures cannot be derived using the method described. Such a problem often arises at latitudes > 50° in summer at ~82-83 km, in the presence of polar mesospheric clouds (PMC) (for more on the PMC from WINDII the reader may consult *Evans et al.* [1995], and for more general background, *Lübken et al.* [1996]). The radiances are expected to be quasi-exponential in form if resulting only from Rayleigh scattering, and therefore the logarithm of the LOS radiances typically satisfies a straight-line criterion. To ensure better SNR and to improve the quality of the data, the columns, which have met the "linearity" criterion in the 75-85 km height range, are averaged into one radiance profile assuming horizontal homogeneity across the WINDII field of view. This increases the image SNR, particularly at altitudes above 85 km where the signal becomes weak because of the exponential decay of atmospheric density.

Further, it was found that the WINDII background radiances do not decrease to zero at high altitudes but instead decrease toward a constant value. *Evans et al.* [1994] suggest that this may be linked to the scattering of sunlight off the lower-altitude cloud layer which is not completely eliminated by the baffle of the WINDII instrument (see *Shepherd et al.* [1993] for more details on WINDII's optical system). Our analysis has shown that the magnitude of this "offset" varies with satellite altitude, local time, and position along the orbit strongly suggesting that it is baffle-scattered light. The problem then becomes how to remove the contamination from the actual radiances. After inverting the LOS radiances to tangent height volume-scattering profiles, the amount of this background signal was evaluated and subtracted out. The retrieved temperatures are quite sensitive to the amount of offset signal removed for the different altitudes. Simulations on the offset amount have shown that a variation of ±10% in the subtracted offset leads to change in temperature of only 0.3% at 65 km, but it increases to roughly 2% at 80 km and under 7% at 90 km. The resulting temperature profiles have a similar shape, but as expected, the larger the subtracted offset is, the cooler the profiles are and vice versa. The effects of the offset value on the temperature retrieved are most pronounced at high alti-

tudes, where the magnitude of the offset removed can be comparable to the magnitude of the actual signal. Some lidar methods [*Whiteway,* 1994] deal with a similar background scattering problem by averaging the signal at high altitudes and then subtracting the average from their photon count profile. In the WINDII case a curve-fitting procedure was applied, where the fitting function relaxes the shape to a second-order polynomial. The minimum value of the fitted curve was selected as the offset value and subtracted from the profile. This method was found to give the most consistent results as is discussed in section 4.

The error associated with the WINDII temperatures can be separated into two categories: the contribution from the quality of the measured data and the contribution from the retrieval routine. The WINDII measurements used in this study are level 1 radiance data, obtained after taking into account instrument responsivity and dark current. The uncertainties associated with these apparent quantities are ultimately carried through the entire retrieval method and determine the accuracy of the resulting temperatures. Comparisons showed that Chahine's inversion on level 1 radiance data is similar to that of pre-processed level 2 data [*Prawirosoehardjo,* 1999], thus the error bounds associated with level 2 background radiance data [*Rochon,* 1999] have been adopted by our retrieval method.

The potential for errors in the radiance inversion scheme can arise from two areas: the ability of Chahine's relaxation to converge to the true solution and the effect of the initial reference profile on the recovered solution. Although, as noted above, the errors from the inversion scheme were taken from level 2 data files, it is still important to recognize and separately evaluate the uncertainties related to Chahine's inversion method. The errors associated with the Rayleigh lidar-style portion of the method come from the influence of the reference pressure profile and from the propagation of uncertainties from the inverted densities, which is called the relative temperature uncertainty. A linear relationship between the input average random noise (in %) and the average temperature deviation (in K) at and below 90 km was obtained with a coefficient of proportionality of 0.826; that is, when an average of 1% noise is added to the input, the average temperature deviation from the noiseless profile is 0.8 K.

The other source of error concerning the inversion technique is the effect of the initial reference temperature profile on the resultant temperatures. The maximum average deviation from the standard profile was found to be < 0.015 K at 65 km, increasing to ~0.3 K at 90 km, and rapidly increasing to 9.3 K at 115 km. The results confirm the notion [*Chahine,* 1972, 1977] that the reference temperature profile has a negligible effect on the retrieved profiles in the altitude range below 90 km.

In the retrieval a model pressure is assigned to the top of each profile to start off the integration. It was estimated that changes in the starting pressure by ±25% led to a temperature difference of only 1.1 K at 90 km which is less than a 1% temperature error, and decreased to < 0.2 K and 0.01 K at 80 km and 65 km, respectively. For the WINDII retrieval algorithm, the reference pressure point is chosen at the top of our image, which is typically 25-30 km above 90 km height.

The relative temperature uncertainty or standard errors for altitudes below 90 km as a function of errors in measurement data, inversion method and reference pressure is calculated after *Chanin and Hauchecorne* [1984]. The uncertainties in the inverted WINDII radiances, or relative densities, were extracted from the matching image in the corresponding WINDII level 2 data file. The analysis showed that at 65 km the temperature error is < 1%, corresponding to an uncertainty of < 0.5% in the measured inverted radiances. At 90 km, where the scatter, is largest the temperature error is of the order of 9-11.5% coming from an error of 5.5-7.5% in the inverted radiances depending on season. All error estimates are summarized in Table 1. The tests were performed on Northern Hemisphere data from 1992 and 1993.

4. Results

Ground-based observations employing Rayleigh and sodium (Na) lidars and falling sphere experiments have the advantage of providing profiles with high temporal and vertical resolution at a given location while satellite observations provide better global coverage. The lidar data presented in the comparisons that follow are limited to middle and high latitudes in the Northern Hemisphere. The falling sphere data are from observation campaigns conducted at northern high latitudes. The retrieved WINDII temperatures are compared to observations from the High Resolution Doppler Imager (HRDI) experiment [*Hays et al.,* 1993] on UARS. Comparisons with CIRA-86 and MSISe-90 are also used as a reference. The WINDII data considered in this study cover a period of 2 years of observations from December 1992/1993, March/April 1992/1993, July/August 1992/1993, September/October 1992, and January 1993/1994, respectively.

WINDII/UARS has only one daytime pass over a given ground-based station per day. Moreover, the WINDII temperature profile is taken within 1.2 s during the day, while most of the ground-based observations are performed at night. Thus, although coincidence can be achieved in terms of location, direct comparison in terms of local time is not possible. To illustrate this point, a comparison of individual temperature profiles from Observatoire de Haute-Provence (OHP) (44°N, 6°E) and WINDII observations closest to the OHP location are shown in Figure 1. As can be seen, the lidar profiles with a 0.3-km height resolution show a more perturbed temperature field than that observed by WINDII. Comparisons of WINDII individual profiles with various ground-based observations inte-

Table 1. Typical Total Temperature Uncertainties for the WINDII Temperatures

Parameter	65 km	70 km	75 km	80 km	85 km	90 km
Retrieved model value, %	<1	<1	<1	<1	<1	<1.5
Relative uncertainty, %	<1	<1.5	<3	<4.5	<7	<11.5
Total uncertainty, %	<2	<3.5	<4	<5.5	<8	<13

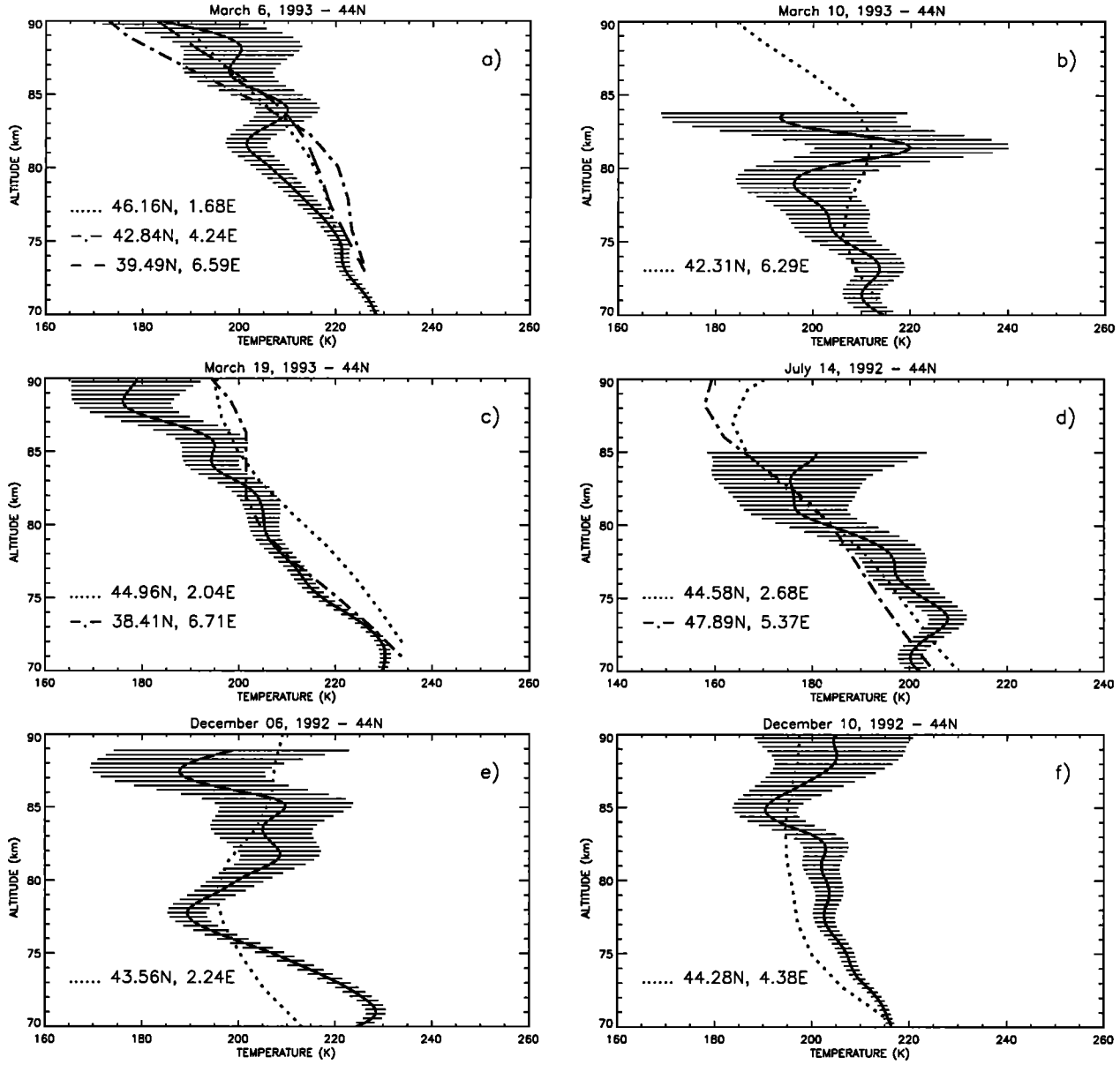

Figure 1. Comparison between individual temperature profiles from OHP (44°N, 6°E) (solid line) and the corresponding WINDII temperature observations taken at the locations indicated.

grated over several hours of local time have also yielded relatively poor results. Thus we have chosen to compare WINDII zonally averaged temperature profiles with nightly averages from the ground-based observations. Such an approach reduces the variability of the individual observations while maintaining the main characteristics of the temperature field.

For each day of observations, individual temperature profiles were retrieved from each image and then binned into 10° latitude bins (e.g., 5°S-5°N, "Equator"; 35°-45°N, etc.), except for 65°-70° N/S, which spans only half of the usual width. Usually two to three individual profiles for each orbit are contained in each of the 10° latitude bins. The difference in local time between these consequent profiles is 1 min on a given orbit. A mean daily temperature profile is created by averaging over all profiles in the latitude bin. On occasion, the satellite makes both an ascending and descending daytime pass during the same day over the same range of latitudes, thus taking measurements at two distinct local times per day. In this case, two separate daily profiles are calculated and treated independently.

Within each daily and monthly average there is a distribution of profiles to be quantified. This distribution represents the short-term daily geophysical variability of the averaged temperatures, and the standard deviation is calculated for all of the altitude bins. Since monthly averages are created from the mean of the daily averages, the geophysical variability of the monthly mean is the standard deviation of the mean; the error bars on the WINDII monthly averaged profiles represent this short-term geophysical variability.

To quantify the difference between two comparative temperature profiles, we calculate the average of the absolute value of the temperature difference between the two data sets. The difference in temperatures at each altitude is calculated and then averaged over all heights in the coinciding measure-

Table 2. Summary of Lidar Data Used in the Comparison

Observation Site	Geographic Location	Type	Time of Observation	Period of Observation	References
OHP	44°N, 6°E	Rayleigh	night	1992-1993	*Singh et al.* [1996]; *see text*
USU	42°N, 248°E	Rayleigh	night	1994-1999	*Wickwar et al.* [1997]
CSU	41°N, 255°E	Na	day/night	1997-1999 1991-1994	*Chen et al.* [2000] *Yu and She* [1995]
URB	40°N, 272°E	Na	day/night	1996-1998 1991-1993	*States and Gardner* [2000a, 2000b] *Senft et al.* [1994]

ment range. This value serves as a measure of correlation between two compared data sets.

4.1. Midlatitudes

Figure 2 shows the comparison of the WINDII temperature profiles with several ground-based lidar temperature observations. The comparisons are in terms of monthly climatological means and include data from Rayleigh-scattering lidars at Observatoire de Haute-Provence (OHP) (44°N, 6°E), France and Utah State University at Logan, Utah (USU) (41.7°N, 248.2°E), as well as from two sodium lidars at Colorado State University (CSU) at Fort Collins, Colorado (40.6°N, 255°E), and Urbana, Illinois (URB) (40°N, 272°E), all situated at 40°-45°N latitude. WINDII temperatures covering 65°-70°N are also compared with observations from Andenes, Norway (NOR) (69°N,16°E). A brief summary, including geographic location, references, and type of observation, is presented in Table 2. A summary of the WINDII measurements used in the comparison with the ground-based lidar observations is given in Table 3 where the number of daily averaged profiles used to create the WINDII monthly mean is given along with the distribution of measurements over the month and the approximate local times of sampling latitude bins. In addition to the experimental data mean monthly values from the CIRA and MSIS atmospheric models at the respective latitudes have been used as a reference.

OHP temperatures shown in this work are monthly averages of temperatures obtained from Rayleigh scattering lidar observations at OHP (44°N, 6°E) in 1992 and 1993 and are available in the NDSC database (A. Hauchecorne, unpublished data, available at http: //www.ndsc.ncep.noaa.gov/ or ftp://ozone.wwb.noaa.gov/ndsc/ohp/lidar/; *Singh et al.* [1996]). A description of the method, which is very similar to that used by the WINDII retrieval algorithm is given by *Hauchecorne and Chanin* [1980] and *Chanin and Hauchecorne* [1984]. The vertical resolution of OHP data is smoothed to 1 km, and it covers an altitude range of 30-87 km; the region of comparison with WINDII is between 65 and 90 km.

Another temperature dataset is that from the Rayleigh lidar at Utah State University (USU) in Logan, Utah, which has data obtained between late 1993 and the present. However, the existing climatology [*Wickwar et al.*, 1997, also Mesospheric temperatures determined from Rayleigh-scatter lidar observations above Logan, Utah: 1. Technique and climatology, submitted to *Journal of Geophysical Research*, 2001; hereinafter referred to as Wickwar et al., submitted manuscript, 2001] is based on only 18 months of data. It appears to reflect strong interannual variability, particularly in winter. A more extensive climatology, based on 1850 hours of data from January 1994 through December 1999, was presented at the Coupling, energetics and dynamics of atmospheric regions (CEDAR) Workshop in June 2000. This data set is used in the comparisons discussed herein. It was derived in a very conservative

Table 3. WINDII Observations Used in the Ground-Based Comparisons

Period	Latitude Bin	Number of Days	Time of Coverage, LT
Jan 1993/1994	35°-45°N	17	0700-1700
March 1992/1993	35°-45°N	22	0600-1800
April 1992/1993	35°-45°N	9	1000-1200, 1700-1900
July 1992/1993	35°-45°N	18	0500-0900, 1500-1800
Aug 1992	35°-45°N	12	0500-0700
Sept. 1992	35°-45°N	8	0700-1100
Oct. 1992	35°-45°N	12	0600-1100
Dec. 1992/1993	35°-45°N	18	0800-1600

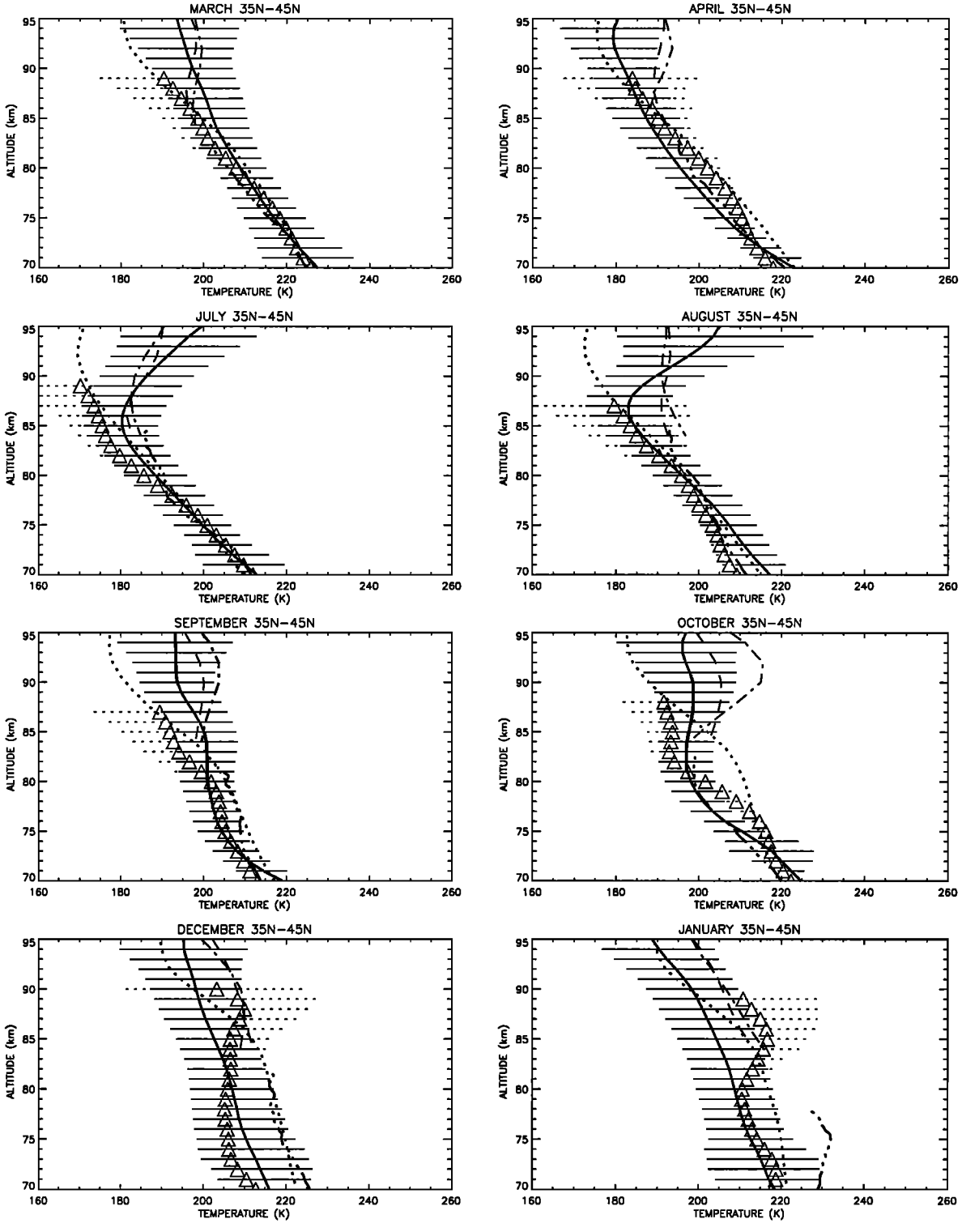

Figure 2a. WINDII temperature (solid line) comparison with OHP (triangles), USU (dash-dot-dot-dotted line), CSU (dashed line), URB (dash-dotted line), CIRA-86 (dotted line). Error bars represent the monthly geophysical variability of the WINDII and OHP measurements.

manner, which limits the top altitudes to 78-84 km. Data reduction procedures are being investigated and refined to increase the maximum altitude by at least 10 km. Results from this more extended climatology will be reported in the near future. The Rayleigh-scatter observations at USU were carried out at 532 nm with a zenith-pointing lidar. Good backscatter data are obtained from below 45 km to above 100 km. For the temperature data reduction the data are averaged over 3 km and 1 hour. The system is described more completely by Wickwar et al. (submitted manuscript; 2001).

While the USU data reduction procedure is based on hydrostatic equilibrium and the ideal gas law, as described in section

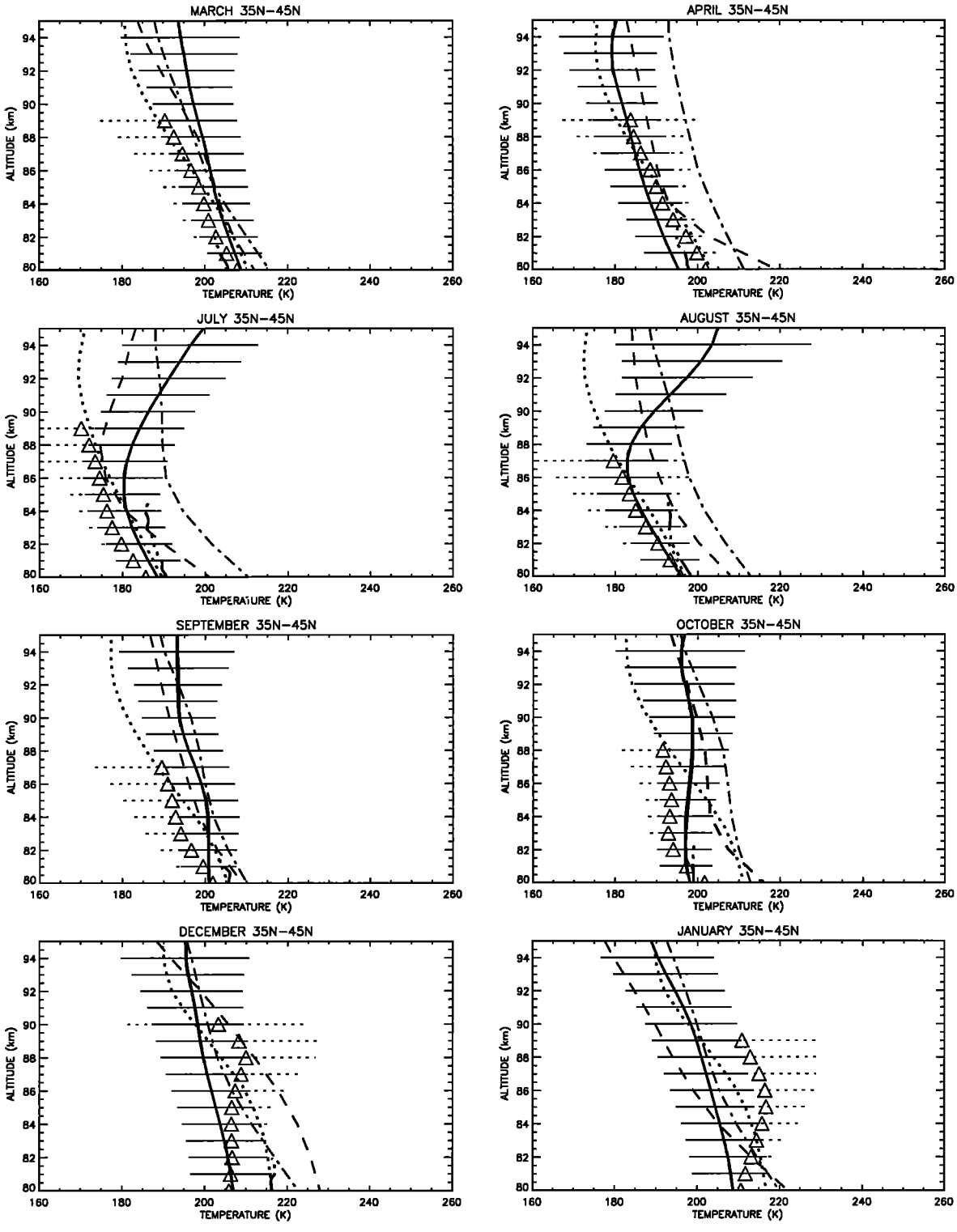

Figure 2b. WINDII temperature (solid line) comparison with CSU (dashed line) and URB (dash-dotted line) diurnally averaged temperatures. The data for OHP (triangles), USU (dash-dot-dot-dotted line) and CIRA-86 (dotted line) are the same as in Figure 2a. Error bars represent the monthly geophysical variability of the WINDII and OHP measurements.

3 and as used for the French lidar data, it differs in detail in the way it was implemented. Near the top of the density profile, where the ratio of signal to standard deviation falls to 16, an initial temperature value, derived from the nighttime temperature climatology obtained from sodium lidar observations at Fort Collins, Colorado [*Yu and She,* 1995], is provided, and a downward integration is performed (Wickwar et al., submitted manuscript; 2001). When the maximum altitude is at or above the lowest altitude in the climatology (between 80 and 83 km, depending on the month), the temporal variation in MSISe-90 is used to account for the day of the month and the midtime of the night's observation. When the maximum altitude is below

the lowest altitude temperature in the climatology for that month, the temperature is extended downward using the shape of the MSISe-90 profile for the appropriate date and time. Assuming this climatological temperature value is close to the correct value, it will have very little influence on the derived temperatures 10 km below the initial point. This procedure was applied to each 1-hour profile for each month. The resultant temperature profiles were then averaged, the uncertainties calculated, and the standard deviations (or RMS variations) determined. Because the altitude of the initial point varies among the profiles being averaged together, the top altitude for the average has been set arbitrarily as the last altitude at which at least half the profiles contribute to the average.

The Rayleigh-scattering lidars can provide temperature measurements up to ~88-90 km height, above which the signal-to-noise ratio rapidly deteriorates and the retrieved temperatures are not reliable. To further validate the upper part of the WINDII temperature profiles, comparisons are made with temperature observations in the altitude range 82-106 km obtained by means of sodium (Na) lidars.

One of the Na lidar data sets used in the comparison are mean monthly temperatures from the CSU lidar facility at Fort Collins, Colorado [*Yu and She,* 1995]. Their climatology evolves from 147 nights of observations with 4 to 11 hours of quality data each night between 1991 and 1993. Temperatures are found by probing the line shape of the Na D_2 absorption line which is dependent on parameters such as temperature and Na density. A more detailed description of the Na lidar setup is provided by *Yu and She* [1995]. CSU temperatures cover the 81-105 km altitude range in 1-km increments. CSU's largest source of error for individual measurements comes from photon noise particularly at the edges of the Na layer. Using hourly averaged temperature profiles, the error at the lower edges of the Na layer at 82 km is 3.4 K and reduces to 0.7 K around the peak of the Na layer approximately at 92 km. The region of comparison is between 81 and 90 km, the range of altitudes where CSU and WINDII measurements overlap.

Recently the sodium lidar at Fort Collins was upgraded to also observe daytime temperatures, allowing the study of a complete diurnal cycle for the period from February 1997 to January 1999, reasonably well distributed throughout the year [*Chen et al.,* 2000]. Comparisons have also been made with these observations and are discussed.

The other sodium radar at Urbana (URB) has been described in considerable detail by *Bills et al.* [1991] and *Bills and Gardner* [1993]. In the current comparison we have used nighttime temperature observations from 65 nights at Urbana with a mean observation period of ~6 hours. The temperature profiles were averaged over the whole observation period and smoothed vertically with a nominal vertical resolution of 1 km [*Senft et al.,* 1994]. Several modifications of the system to permit daytime observations were addressed by *Yu et al.* [1997]. These modifications led to the acquisition of more than 1000 hours of lidar observations from February 1996 to January 1998, approximately uniformly distributed throughout the diurnal and annual cycles [*States and Gardner,* 2000a, 2000b]. The range of comparison with WINDII is from 84 km to 95 km for the nighttime observations by *Senft et al.* [1994] and *Yu and She* [1995], and from 80 to 95 km for the diurnal mean temperatures by *States and Gardner* [2000a, 2000b] and *Chen et al.* [2000].

The comparison with the ground-based lidar observations is presented and discussed in parallel between the WINDII daytime observations and ground-based nighttime averages on one hand, and WINDII daytime and ground-based diurnal averages, on the other. The comparison with the nighttime data, conducted for selected months from January to December, is given in Figure 2a; here the error bars in the WINDII profiles indicate the geophysical variability of the WINDII monthly means.

4.1.1. March/April. In March, WINDII is in good agreement with the OHP 1992/1993 monthly mean temperatures (triangles) below ~80 km, and the lower segment of the sodium lidars between 85 km and 95 km. There is also good agreement with USU (dash-dot-dot-dotted line) and CIRA (dotted line) up to 84 km. The WINDII daytime temperatures are warmer than the USU and OHP nighttime observations by ~3.5 K above 80 km. The comparison with the URB nighttime observations [*Senft et al.,* 1994] (dash-dotted line) and CSU [*Yu and She,* 1995] (long dashed line) up to 90 km shows a reasonably good agreement with the WINDII temperatures with the latter being warmer by 3.5 K at the bottom of the Na lidar profiles, but above 90 km altitude the CSU/URB profiles become warmer than WINDII by the same amount, yet still within the WINDII geophysical variance. In April the agreement is good with USU and to some extent with OHP, although WINDII is colder than all lidar observations considered. In the two spring months, there appears to be a temperature minimum in CSU's data at ~86 km which *Yu and She* [1995] interpreted as a double-minimum mesopause structure: one minimum around 86 km and the other around 99 km (not shown here), associated with the equinoctial transition between the high-winter and low-summer mesopause state.

A comparison with the diurnally averaged (day and night measurements) temperatures by CSU [*Chen et al.,* 2000] and URB [*States and Gardner,* 2000a, 2000b] for March, given in Figure 2b, shows that they agree well with the WINDII temperatures up to 85-87 km height, where there is a node between WINDII and CSU/URB profiles. Above that altitude WINDII temperatures are warmer than CSU and URB being still within the WINDII's variance range, in agreement with results reported by *Chen et al.* [2000]. At 95 km the difference is of 5 K for CSU/URB. There is a very good agreement with the URB (dash-dotted line) diurnally averaged temperatures shown in Figure 2b, in March with actual values differing by < 1 K between 83 and 87 km. In April, both CSU and URB diurnal temperatures are systematically warmer (that is, they fall outside the range of WINDII's geophysical variance) than WINDII above 84 km by 4 K and 15 K, respectively. Below 85 km, however, the difference with CSU rises to ~22 K at 80 km, but as this is the lower boundary of the Na lidar the measurements are affected by the large standard deviation of the lidar measurements. All compared data sets except for URB are within the WINDII geophysical variances in the 70 to 95 km altitude range but as in the comparison with the nighttime observations, shown in Figure 2a, the WINDII April temperatures are colder than CSU/URB. The reasons for these differences might be associated with the effect of the springtime transition on the mesospheric temperature fields as is discussed in detail by *Shepherd et al.* [2001]. Also, because of the UARS yaw period the WINDII April data are taken from only about a week of observations at the end of the month in both 1992 and 1993, thus representing only 2 to 4 hours of local time; therefore they could be significantly biased by the diurnal tide.

4.1.2. July/August. Very good agreement between USU and CSU nighttime observations and WINDII is seen in July in Figure 2a with an average difference of < 3 K in the height

range 70-95 km with deviations between CSU and WINDII of < 2 K in the mesopause region at ~86 km. The USU observations are in excellent agreement with WINDII up to ~80 km. There is a very good agreement between the top of the USU profile and the bottom of the URB profile, as can be expected from the USU retrieval, forming a combined profile with a minimum of 182.5K at ~88 km compared to the low July mesopause at 86 km with temperature of 180 K observed by WINDII. Above 87 km the OHP standard deviation becomes significant for temperatures very close to the CIRA model predictions and it is difficult to determine the height of the mesopause in the July 1992/1993 OHP data. The mesopause seen by WINDII is at a lower altitude and warmer by ~20 K than that predicted by MSIS/CIRA. The mesopause heights observed by both data sets fall within the range of altitudes observed by *She and von Zahn* [1998] using midlatitude lidar. The WINDII mesopause temperature is also in good agreement with the value reported by *She and von Zahn* [1998] of ~173 K for the summer mesopause at midlatitudes after allowing for daytime/nighttime variability of 6 K due to diurnal tide perturbations [*States and Gardner,* 2000a, 2000b]. More about this is said in section 6.

The CSU July nighttime data between 82 and 105 km (Figure 2a) show a temperature minimum corresponding to the mesopause at 86 km with a temperature of 181 K, which is comparable to WINDII's July mesopause temperature of 180 K at that height. Above 90 km both CSU and URB are colder than WINDII with a difference reaching 10 K at 95 km height; at 90 km WINDII agrees well with the CSU nighttime temperatures but is colder than URB by 5 K. There is a good agreement between USU and URB July/August temperatures at 85 km where the two profiles overlap. The OHP data also agree well with USU up to 80 km. There is an excellent agreement between WINDII and CIRA up to 86 km and WINDII and OHP between 77 and 87 km with WINDII being slightly warmer. The agreement between USU and CSU is also good at the overlapping height of ~85 km; WINDII is warmer than USU up to 77 km, but becomes colder than USU with increasing height and at 84 km (the top of the USU August temperatures) the difference is of the order of 6 K. With respect to the OHP observations, WINDII is warmer by 2-7 K below 78 km and in excellent agreement above that height. As in the July case the URB and CSU data are significantly colder than WINDII above 90 km. However, we cannot put much significance on this difference since at these altitudes the quality of the WINDII data deteriorates because of decreasing SNR. We remind the reader that in the current version of data processing the WINDII temperatures are most reliable below 90 km height. The WINDII temperatures appear colder than both nighttime Na lidar climatologies in the 85-90 km height range.

Large differences between WINDII and the URB and CSU's diurnally averaged temperatures in July (Figure 2b) are evident particularly at 80 km, where the differences are ~22 K for URB and ~13 K for CSU which are comparable with URB's large daytime RMS errors of 21.5 K at 80 km. The temperature difference then decreases with height. The height of the WINDII mesopause is at 85-86 km, while the CSU diurnally averaged temperatures suggest a mesopause at ~88 km. The WINDII temperatures are between the CSU and URB diurnally averaged temperatures in July, being warmer than CSU by 5 K and colder than URB by 15 K. In August the mesopause according to the WINDII data is at 87 km, while both Na lidar data sets indicate a mesopause above 95 km.

According to *States and Gardner* [2000a] the diurnally averaged temperatures show the mesopause in its high-altitude state (98-101 km) until May 7; thereafter it descends to 86-88 km until July 15 when it is seen to jump back to 96 km and then continually increase with height as winter approaches. This suggests that the daytime data show the abrupt lifting of the mesopause in mid-July. Alternatively, when *States and Gardner* [2000a] average only their nighttime data, the low summer time mesopause is present between April 9 and August 12. The mesopause height according to the WINDII daytime observations at 35°N-45°N suggests that globally the pattern is more consistent with *States and Gardner*'s [2000a] nighttime observations. Most of the July 1992/1993 data are for dates from July 15 to August 23. The differences between WINDII and CSU and WINDII and URB at 86 km in August are 7 K and 15 K, respectively, with WINDII being consistently colder than the Na lidar observations.

4.1.3. September/October. In September, WINDII is colder than the USU data sets (Figure 2a) and agrees well with OHP up to 80 km. At altitudes above 85 km, WINDII is colder than both Na lidar profiles. With respect to CIRA, WINDII is colder below 83 km and warmer above that altitude. The profile indicates two broad temperature inversions with a minimum at ~75 km and 90 km, respectively. A large part of the compared nightly averaged temperatures are within the range of the WINDII daytime variability as can be seen from the corresponding plot in Figure 2a. In October the comparison with USU, CSU, URB, and CIRA gives less satisfactory results. The WINDII monthly average shows two local minima at 80 km and possibly 94 km, although the latter might be also an artifact of the data at that altitude. WINDII agrees well with the USU (dash-dot-dot-dotted line) observations and is colder by 7 K than CSU (long dashed line) at all corresponding heights up to 90 km.

In terms of the comparison between WINDII and the CSU/URB diurnal averages for September (Figure 2b) the WINDII temperatures are warmer than CSU on average by ~4 K and colder than URB. Both CSU and URB daily averages are within the WINDII geophysical variability range. As with the nighttime data in October (Figure 2a) the comparison with CSU and URB is less satisfactory.

4.1.4. December/January. In December and January the CSU observations suggest a warmer upper mesosphere than that observed by WINDII and predicted by CIRA (temperature difference of 6 K at ~77 km in December). The large geophysical variabilities (standard deviation) in the USU winter temperatures might be related to inversion layers in the individual profiles caused by gravity and planetary waves. These values reach ±18.2 K in January and ±14.4 K in December at 77 km (not shown here) compared to ±7 K seen by WINDII at the same height. In comparing temperature errors, USU temperature uncertainties are very similar to those for OHP (0.5 K at 70 km, and 1 K at 77 km). Earlier observations by *Wickwar et al.* [1997] indicate that interannual variability in the magnitude and height of the inversion layers could add to the climatological variability. Another possible reason for the large variability in the USU data especially in the January case, might be the mountain topography of the lidar site leading to an increase in gravity wave activity. The differences between the WINDII daytime observations and the nighttime lidar temperature observations are of the order of 6-7 K at altitudes below 85 km and 10-12 K above that height, thus being consistent with the diurnal variability reported by *States and Gardner* [2000b] and *Chen et al.* [2000].

In December the combined CSU/URB/USU nighttime pro-

file (Figure 2a) is warmer than WINDII by 9 K at all altitudes, from 70 to 95 km. Similar differences are seen in January above 85 km between WINDII and CSU and URB, with the latter being warmer than WINDII by 9 K. In January, OHP agrees with the WINDII data below 80 km and with the URB temperatures above 85 km. There is a distinct temperature inversion in the OHP profile with a minimum at ~79-80 km height. The fact that our temperatures decrease continually between 70-90 km is consistent with a high winter mesopause, above 90 km. When WINDII is compared with the diurnally averaged temperatures from CSU and URB (Figure 2b) the agreement is better with the URB observations at 85-95 km than with CSU, especially for the January case.

The review of the comparisons in Figure 2 shows that the OHP 1992/1993 data revealed a more vertically structured nightly temperature field, particularly in the October-January comparisons than is derived from the WINDII observations. *Hauchecorne et al.* [1991] suggest that this arises from temperature inversion events which are more frequently observed in the wintertime and add to the variability in the data sets. While this might also be the cause of WINDII's large geophysical variability, part of our large wintertime variabilities may also be attributed to a smaller number of profiles making up the December (18 profiles) and January (17 profiles) averages. In comparing temperature uncertainties, typical OHP temperature errors are reported to be < 1 K (0.3%) at 70 km, a 3 K (1%) error at 80 K, and a 10 K (3%) temperature uncertainty at 90 km [i.e., *Hauchecorne et al.*, 1991]. The typical WINDII uncertainties in the derived individual temperature profiles at the same altitudes are 1.5%, 4.5%, and 11.5%, respectively. For the monthly averages this error is significantly reduced by $\sqrt{N}$, where N is the number of individual profiles included in the average. Although it seems that the WINDII errors are about twice as large as those of OHP, the agreement is still very good. Even with large temperature differences in the winter, the maximum geophysical variability of both measurements coincides at most heights.

In the comparison with Na lidar observations two distinct patterns have emerged with respect to the WINDII data: (1) small differences between the compared data sets within the range of the WINDII standard deviation of the monthly means (i.e., Figure 2a, March, July; Figure 2b, March, September) and (2) large differences when WINDII is colder than the lidars at all altitudes above 85 km (Figure 2a, April, August December, January). The nature of these large differences appears to be systematic and is currently being investigated. Systematic differences can occur through the sampling. Lidars measure the same atmosphere at the same location and integrate over the whole night (or day and night). WINDII uses zonal averages which reflect the whole globe and samples different local times on different days of the month. Another source of systematic error lies with the subtraction of the offset as was mentioned in section 3. The offset is determined at altitudes above 95 km where the SNR rapidly decreases. Assuming a temperature of 190 K at 95 km, 10% error in the subtracted offset would give a temperature difference of 13.3 K, which will put, for example, the WINDII April temperature profile between the CSU and URB data.

The results from the WINDII/lidar comparison at midlatitudes have shown that more often than not there is a satisfactory to very good agreement of the WINDII daytime temperature observations with nighttime averaged temperatures but that the agreement is not better with the diurnally averaged values. This suggests that the thermal diurnal tide does not significantly bias the results obtained. In a recent study, *States and Gardner* [2000b] have shown that the atmosphere below 92 km height is subjected to strong diurnal variation throughout a great part of the year, with the exception of late November, December, and early January, when the diurnal amplitude is small throughout the mesopause region. The average temperature amplitude is found to be relatively stable at 6.1 K from spring to autumn and at 3.8 K for winter. The comparison of the annual background temperature by *States and Gardner* [2000b] shows that at an 85-km height, depending on the local time of the WINDII daytime observations, the difference with the ground-based nighttime data at 80-85 km could be as much as 10 K for a midnight-noon comparison, 7 K for midnight-early morning (0600 LT) and 4 K between night and early evening (1800 LT).

The comparisons presented so far have shown that there is apparent seasonal variability in the magnitude and shape of the mesospheric temperature profiles considered. To examine further how well the WINDII temperatures reflect the seasonal variabilities with respect to the lidar observations, the WINDII daily zonal mean temperatures at 87 km in 1992 are compared with nightly averaged temperature measurements at the same altitude from CSU (C.Y. She, unpublished data, 2000) and OHP in the same year. The CSU temperatures are obtained by first averaging hourly mean photon profiles, then calculating hourly mean temperatures, from which the nightly average temperature values are obtained. The CSU temperatures used in this comparison are at 87±1.8 km height. The results of this comparison are shown in Figure 3 together with the annual variability curve approximated as a cosine wave (mean temperature of 197 K, amplitude of 24 K, and phase of 351 days, adapted from *Chen et al.* [2000]) to guide the reader's eye.

In the spring the WINDII temperatures (triangles) are in reasonable agreement with the CSU observations (squares) and OHP (solid circles), as they appear to be similar to or a few degrees warmer than those for the lidar. The WINDII temperatures are well distributed along the annual variability curve. In July (days 183-213) the WINDII temperatures appear warmer than OHP and the annual fit but are in the range of the available CSU observations. In August (days 214-244), there is very good correspondence between WINDII, OHP, and the annual fit. In mid-September (day 260), WINDII is much colder than the seasonal variability, but there are no lidar data to confirm that our measurements are correct. Still, the WINDII values appear rather constant for the 3 available days. The available CSU temperatures for the beginning of September are higher than the annual values. After these 3 days the WINDII temperatures quickly return to the annual values and stay within that range until mid-October before decreasing by ~17 K in agreement with the OHP observations. In general, the observed temperatures from late October until December appear very perturbed and do not comply with the annual fit, although they agree well with each other. In general, there is better correlation on a day-by-day basis between the OHP and WINDII observations than between CSU and WINDII. An interesting result from the comparison is the much colder temperatures of the three data sets in October/December than reflected in the cosinusoidal seasonal variability. Figure 3 has shown that the WINDII temperatures adequately reflect the range and pattern of seasonal and day-to-day variability observed by the midlatitude lidars in spite of the potential diurnal tidal bias of the of the daytime/nighttime observations.

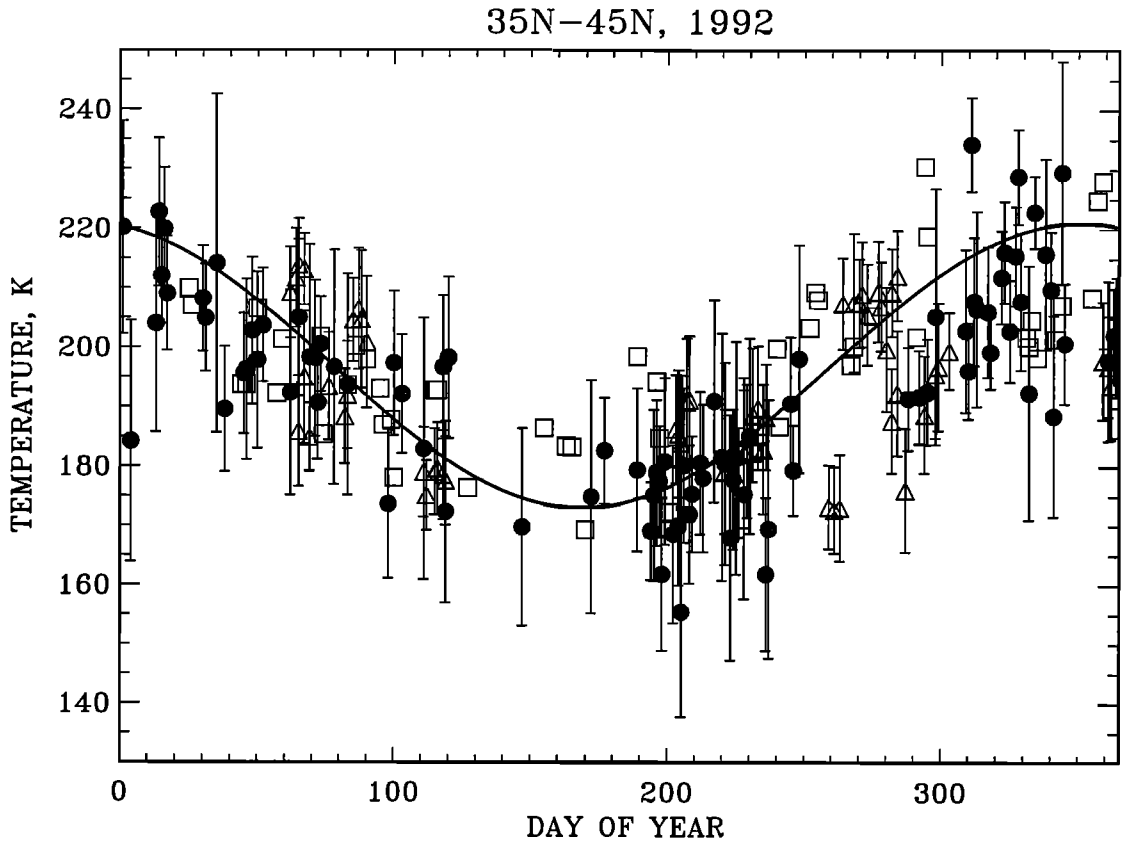

Figure 3. Comparison of WINDII daily zonal means (triangles) with nightly averages lidar temperatures from CSU (squares) (C.Y. She, unpublished data, 2000) and OHP (solid circles) for 1992 at 87-km height.

4.2. High-Latitude Comparisons

Observations of mesospheric temperatures at high latitudes in the Northern hemisphere have been conducted at Andenes, Norway [*von Zahn and Meyer,* 1989; *Lübken and von Zahn,* 1991; *Lübken,* 1999] by means of a sodium lidar and complemented by falling sphere observations. The data analyzed sporadically cover 1980 to 1993. In the 40-85 km height range, data are recovered by falling spheres overlapping with Na lidar data ranging between 80 and 110 km. Smoothed monthly mean temperatures for March, July and December are available between 50 and 92 km in 1 km increments. These NOR temperatures are compared with WINDII temperature zonal mean averages at 65°-70°N latitude, and some of the results are shown in Figure 4. The typical geophysical variabilities of the lidar data range from 6 to 14 K in March and from 9 to 20 K in December. As before mean monthly values from CIRA-86 (dotted lines) and the fifteenth of the month from MSISe-90 (dashed lines) are also plotted. In March the temperatures from 28 days of Na lidar observations and 6 days of FS measurements are compared with the WINDII daytime temperatures. The average temperature difference between NOR and WINDII in the height range 74-90 km is 5.3 K. The best agreement

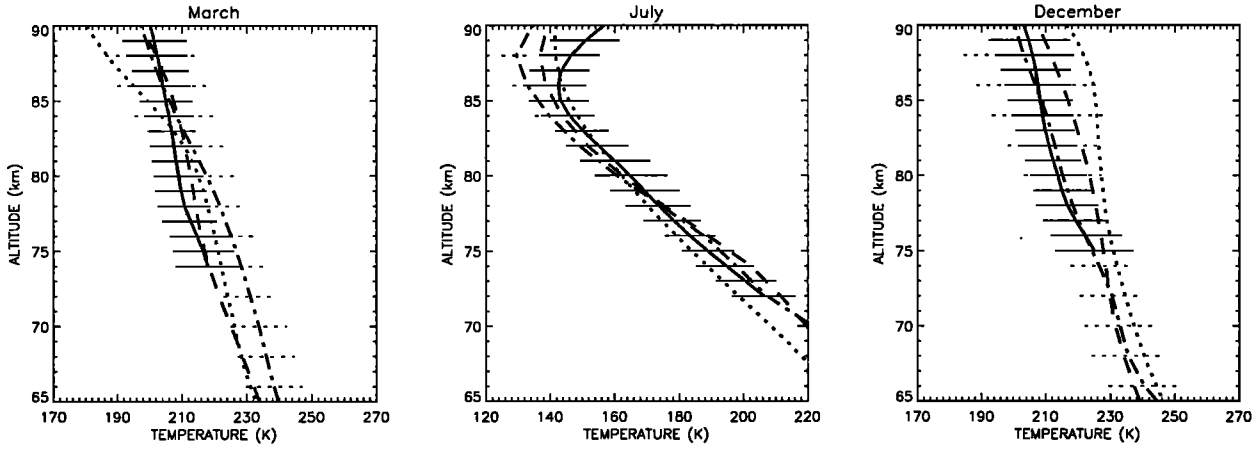

Figure 4. WINDII temperature (solid line) comparison with NOR (dash-dotted line), CIRA-86 (dotted line) and MSISe-90 (dashed line). WINDII monthly averages cover 65°-70°N. Error bars represent the monthly geophysical variability of the WINDII (solid line) and NOR (thin dots) measurements.

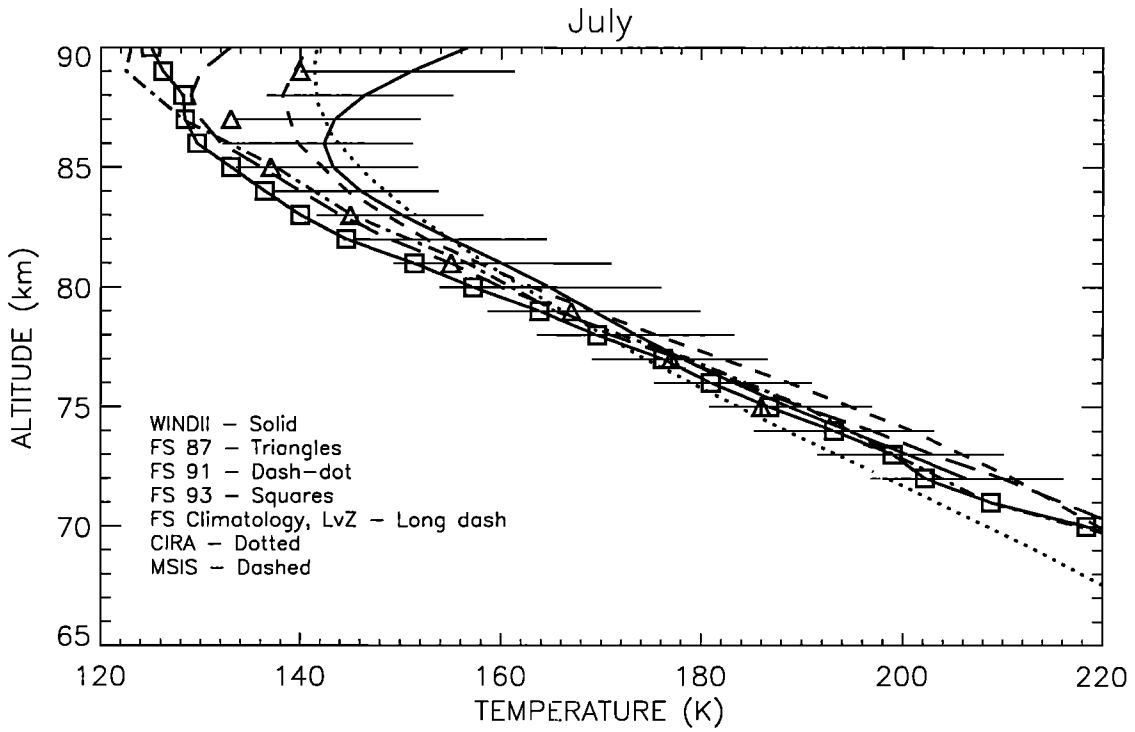

Figure 5. July WINDII temperatures (solid line) between 65°-70°N compared with falling spheres and model data at Northern polar latitudes: CIRA-86 (dotted line), MSIS90 (dashed line), FS-87 from [*von Zahn and Meyer,* 1989] (triangles) and FS profiles from campaigns in 1991 (dash-dotted line) and 1993 (squares/solid) (F. Schmidlin, personal communication, 1995), and FS climatology profile [*Lübken and von Zahn,* 1991; *Lübken,* 1999] (long-dashed line). Error bars represent the monthly geophysical variability of the WINDII measurements.

is above 85 km, where the differences are less than 2 K. For this month, WINDII has the best agreement with MSISe-90. Comparisons in December (7 days of Na observations and 5 days of FS) are very good with absolute average differences of 2.1 K in December. During the winter, both lidar and WINDII generally report cooler temperatures than do either of the models. The winter mesopause is observed to be at ~96 km, thus being outside the WINDII range of reliable retrieval. As in the comparison with the OHP and USU data sets, the variability in the NOR profiles is largest in the wintertime, reflecting temperature fluctuations possibly caused by gravity and planetary waves [*Lübken and von Zahn,* 1991]. Comparisons in the springtime and wintertime are reasonable with the maximum variability of the two data sets overlapping at all coinciding heights below 90 km.

The comparison with falling spheres (FS) at 69°N latitudes employs two type of data. First there are temperature profiles reported by *von Zahn and Meyer* [1989], *Lübken and von Zahn* [1991] and *Lübken* [1999]. In addition, 13 individual FS profiles measured at 68°N in Kiruna, Sweden in late July and early August of 1991 and 1993 have also been considered (F. Schmidlin, personal communication, 1995). The FS technique involves deploying an inflatable falling sphere at ~110 km in altitude and accurately tracking its passive fall towards the Earth using high precision radar [*Lübken et al.,* 1996]. The motion of the sphere can be described using simple equations of motion from which one can derive atmospheric density and wind velocities [i.e., *Schmidlin et al.,* 1991]. Temperatures can then be found in a similar fashion to Rayleigh lidar. Figure 5 shows the comparison at 65°-70°N of the WINDII zonal mean temperatures (solid line) for July with FS-87 temperatures (triangles), FS temperature measurements at Kiruna from campaigns in 1991 (dash-dotted line) and 1993 (squares/solid line), FS climatology [*Lübken and von Zahn,* 1991; *Lübken,* 1999] (long-dashed line), July CIRA-86 (dotted line) and MSIS90 (dashed line) values at 70°N. Typical summertime variabilities for FS-87 are between 4 and 6 K. The summer mesopause by WINDII is found to be at 86.3 km with a temperature of 142.5 K. According to CIRA, FS-91, and FS-93 the July mesopause is found at 90 km with temperatures of 141.8 K and 122.5-125 K, respectively. However, the FS climatology profiles summarized by *Lübken and von Zahn* [1991] and *Lübken* [1999] indicate an average mesopause height at 88 km with temperature of 129 K. The average temperature difference with MSIS between 75 and 90 km is 4.8 K. In general, high-latitude summertime WINDII data are in good agreement with FS and MSIS data up to ~86-88 km where we observe a lower and warmer mesopause. The FS data are, however, within the WINDII standard deviations. The WINDII temperature profile also agrees with the characteristics of a single, low and cold summer mesopause predicted by *She and von Zahn* [1998] at polar latitudes. A possible contribution to the disagreement with the FS data may be the fact that only 15 individual profiles were used to generate the FS-87 dataset and 13 individual profiles were obtained during the FS-91 and FS-93 campaigns. In comparison, 196 individual profiles between 65° and 70°N were used to create the WINDII zonal mean profiles for July. More significantly, all FS observations were performed in the presence of polar mesospheric clouds where WINDII results are discarded. WINDII, FS, and the models are all in good agreement below 82 km, the mesospheric region below the observed cloud bases of NLCs and PMCs.

4.3. Satellite Comparisons

WINDII monthly mean temperatures are also compared with observations from the High-Resolution Doppler Imager (HRDI) aboard the Upper Atmosphere Research Satellite (UARS). Comparisons with other satellite instruments are important as they perform data reduction/processing techniques similar to our analysis and allow a wider range of global coverage and comparisons. For example, a comparison with the ISAMS [*Taylor et al.*, 1993] experiment on UARS using an earlier version of the WINDII temperature retrieval by *Shepherd et al.* [1997] showed that most of the compared WINDII temperature profiles (expressed as radiances not corrected for local thermodynamic equilibrium) agreed within 5-10 K with ISAMS below 85 km and were within the range of the instruments' experimental errors. In addition, the HRDI values are also daytime values.

For the purposes of the current comparison, WINDII average temperature profiles have been binned over a 10° latitude surrounding the latitude given by the HRDI instrument; for example, the 30°N temperature profile from HRDI is compared with a WINDII average produced using profiles in the range of 25°-35°N.

The HRDI temperatures are recovered through rotational temperature measurements of the O_2 atmospheric band spectra. A full description of HRDI's retrieval method, error analysis, and preliminary results for July 1993/1994 is provided by *Ortland et al.* [1998]. HRDI temperatures (dash-dotted lines) for 0°, 30°, 45°, and 60°N are plotted against WINDII July averages (solid lines) in Figure 6. The number of profiles included in the WINDII average is listed in Table 4. The comparison shows that HRDI summer temperatures are generally colder than WINDII at equatorial and Northern midlatitudes. The agreement with HRDI increases poleward as at 45°N and 60°N the average deviations fall to 2.2 K and 1.5 K at the corresponding latitude bins. At lower latitudes the disagreement stems from HRDI's observation of a double minimum at roughly 80 and 98 km (the latter is not shown here). At 45°N the double minimum can still be seen but the lower one at ~83 km is colder than the higher altitude minimum. At 60°N, only one temperature minimum is seen around 86 km in agreement with the WINDII observations at 40°-50°N at 84.3 km and at 84.6 km between 55° and 65°N. The mesopausal temperatures also correspond well; WINDII temperatures are 173.1 K and 152.4 K at 40°-50°N and 55°-65°N, while HRDI temperatures are 172 K and 156 K respectively. HRDI's observations generally support *She and von Zahn's* [1998] theory that during the summer the mesopause remains in a high altitude state in the tropics but lowers in height by midlatitudes and becomes progressively colder toward the poles. This pattern is not as clear in the WINDII data, mainly because we are restricted to altitudes below 90-95 km. Overall, the agreement between HRDI

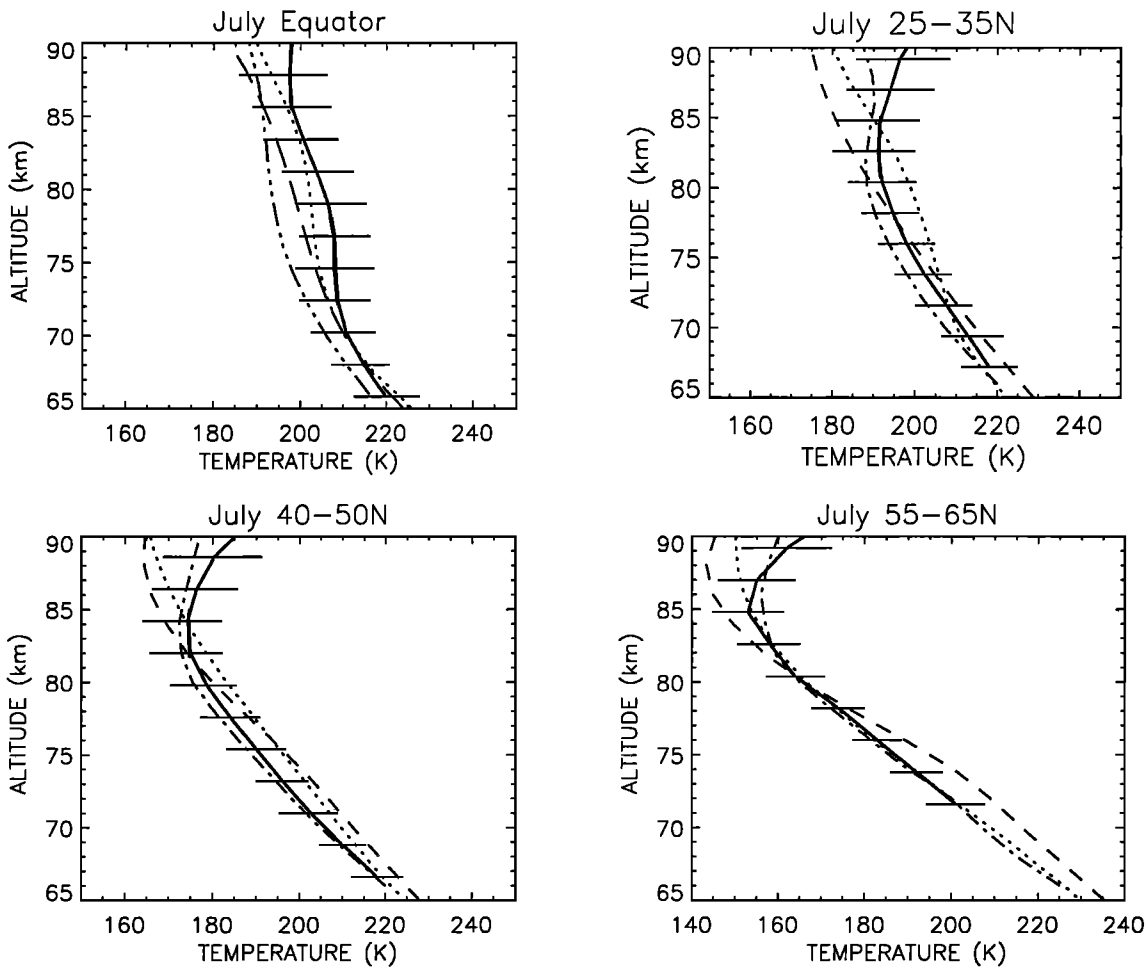

Figure 6. July WINDII temperatures (solid line) compared with HRDI temperature (dash-dotted line). July CIRA-86 (dotted line) and MSISe-90 (dashed line) values are also plotted.

Table 4. WINDII Data for Comparison with HRDI, as Is Shown in Figure 6

Latitude Bin	July	
	Time Coverage, LT	Number of Days in Monthly Mean
5°S - 5°N	0500-0800, 1700-1800	12
10° - 20°N	0500-0800, 1600-1800	14
25° - 35°N	0600-0900, 1500-1900	17
40° - 50°N	0700-1000, 1500-1900	22
55° - 65°N	0900-1100, 1400-1900	13

and WINDII is very good, particularly at northern middle to high latitudes.

The WINDII temperatures have been also compared with temperature observations by the Solar Mesospheric Explorer (SME) experiment [*Clancy and Rusch,* 1989; *Clancy et al.,* 1994] conducted between January 1982 and September 1986. The SME's sun-synchronous orbit limits the local coverage of the observations around 1500 LT for three to five widely separated longitudes in the Western Hemisphere. The results from the WINDII/SME comparison for the corresponding local times and longitudinal range are part of another study which is currently under way and will be reported upon in the near future.

5. Discussion

For all data sets the agreement is best for the month of July for three possible reasons. First, the summer months are reported to have the lowest geophysical variability [*Lübken and von Zahn,* 1991; *Wickwar et al.,* 1997] at middle and high latitudes. Planetary waves are more easily able to propagate into the winter mesosphere, unlike the summertime when they interact with the westward mesospheric jet and are more commonly filtered out. As a consequence, winter time measurements are characterized by more frequent temperature inversion events, thus adding to the variability observed. This is supported by the WINDII, OHP, and USU observations as was already mentioned. In terms of the mesopause temperatures below the 90-km limit presently imposed for WINDII data reliability, July is the only month in our data set when WINDII can widely view the low summer state mesopause at middle and high latitudes. In summer, poleward of ~40°, the mesopause is reported to descend to its low-altitude state [*She and von Zahn,* 1998; *Ortland et al.,* 1998] where WINDII can obtain information on its height and temperature. The mesospause height may be used as another characteristic of comparison. Further, in July there is a wide range of measurements available over a wide range of latitudes, particularly in the Northern Hemisphere, making the validation of the WINDII observations more complete.

Several final items worthy of mention are *States and Gardner*'s [1998, 2000b] findings concerning mesosphere inversion layers and how data sampling can bias the interpretation of the retrieved temperatures. They suggested that incomplete sampling of tidal perturbations may be partially responsible for the inversion layer frequently observed near 70 km in nighttime temperature profiles obtained by Rayleigh lidars [e.g., *Leblanc and Hauchecorne,* 1997; *Meriwether et al.,* 1998; *Wickwar et al.,* 1997]. It was also suggested that if measurements were averaged over a complete 24 hour period then evidence of diurnal tides (and thus temperature inversion layers) would effectively disappear. *States and Gardner* [1998] also suggest that tidal interaction with planetary and gravity waves could also play important roles. *Hauchecorne et al.* [1987] report that inversion layers have been seen to persist for several consecutive days and for many consecutive hours during a single night. It was suggested that these events may not only be generated by diurnal tides but also potentially by the breaking of gravity waves. So while diurnally averaged temperatures may suppress the effects of tidal activity, the effects of breaking gravity waves could still appear in daily and monthly averaged temperature profiles. Our experience with the WINDII data set has shown that temperature inversions at 75-80 km are often seen in the daytime temperature profiles and persist for a few days at equatorial and midlatitudes. The physical mechanisms behind mesospheric temperature inversion layers have been thoroughly discussed [e.g., *Leblanc and Hauchecorne,* 1997; *Meriwether et al.,* 1998; *States and Gardner,* 2000a, 2000b; *Chen et al.,* 2000]. *States and Gardner* [2000b] observed significant differences between diurnally averaged temperature profiles and nighttime-only averaged profiles. For example, URB's nighttime-only data show a July mesopause averaging around 178 K, while their diurnal average shows a much warmer value of 187 K. Preliminary results from recent diurnal measurements at CSU show that their diurnally averaged mean summer mesopause temperature is virtually the same as the one calculated using nighttime only data [*Chen et al.,* 2000], suggesting that the differences due to the diurnal tides are small. For the altitude region between 80 and 105 km, *Chen et al.* [2000] report that their nighttime annual mean temperatures are colder than the diurnal mean by no more than 2 K below 88 km and warmer by no more than 3 K above that height. The largest differences between annual daytime and nighttime averages were reported to be between 4 and 6 K. Differences of this magnitude are well within WINDII temperature uncertainties and our calculated geophysical variabilities. This is consistent with the fact that WINDII daytime temperatures also correlated well with other nighttime data, particularly when our daily averages were well sampled in number and covered a broad range of local times (e.g. March between 35° and 45°N). It is clear that more diurnal observations of the mesosphere are needed to resolve the influence of different wave perturbation on the climatological averages and to help better understand the processes in the upper mesosphere. A compilation of WINDII daytime data combined with the large

database of nighttime lidar observations could also be used to serve that purpose.

6. Conclusions

WINDII temperatures from January 1993/94, March and April 1992/1993, July and August 1992/1993, September and October 1992, and December 1992/1993 have been compared with a number of ground-based and spaceborne temperature observations at several latitudes in the Northern Hemisphere. The purpose of the comparisons was to provide a consistency check of the retrieved values to facilitate future scientific analysis. This was carried out in the light of the error budget estimates performed on the retrieval routine to provide independent measure of the accuracy of the retrieved temperatures. However, it soon became apparent that the necessary differences in the way ground-based and satellite data are averaged are critically important. For this reason the WINDII comparisons were conducted in four different ways: comparisons of individual profiles, comparisons of daytime/nighttime and diurnally averaged data, and comparisons of daily zonal means to examine seasonal and latitudinal variability.

1. The comparison of individual daytime satellite and lidar nighttime temperature profiles has shown that good agreement is rarely achieved because of the differences in the spatial and temporal sampling of the atmosphere. This problem was encountered also during the validation of the wind measurements by WINDII and HRDI, when hundreds of measurements over a given ground-based site were required in order to yield scatterplots showing a meaningful correlation [i.e., *Gault et al.*, 1996].

2. The comparison of monthly averages obtained from daily zonally averaged WINDII temperatures with monthly temperature means from different ground-based lidar facilities showed that in spite of potential diurnal tidal biasing both in the WINDII and lidar observation, often there is better agreement of the WINDII daytime observations with the lidar nighttime averages than with the diurnally averaged values. However, since the diurnally averaged temperatures are available only for the last couple of years, this lack of agreement may arise from interannual variability. If so, this means that the interannual variability is greater than that of the diurnal tide. However, while for the months of March, July, and September the agreement is particularly good, the differences for April, October, December, and January fall at or outside the WINDII limits of geophysical variability. These systematic differences can arise from differences in the sampling, or possibly in the WINDII baffle-scattering correction.

3. Examining the seasonal variability of the WINDII and lidar temperatures at midlatitudes showed very good correspondence between the WINDII observations and the sodium and Rayleigh nighttime lidar observations. An interesting feature is the agreement between the three data sets in late autumn and early winter, when in addition to the large local variability seen in the lidar data the observed temperatures are colder by ~10 K than the smooth annual variability, suggesting a transient perturbation following equinox.

4. The comparison between WINDII and ground-based and falling spheres profiles at high latitude have shown that the WINDII observations reflect well the mesospheric temperature field in summertime at these latitudes and can successfully be used to study the atmosphere in the vicinity of such phenomena as polar mesospheric clouds observed in summertime at high latitudes.

5. Finally, the comparison of temperature profiles obtained in daytime by two different experimental techniques aboard the UARS satellite have shown that the WINDII and HRDI temperature data sets are comparable to each other for latitudes above ~20° latitude in observing the temperature field of the upper mesosphere and the mesopause region. Differences at the equator are not understood.

The results of our analysis presented in this paper have shown that data from the Wind Imaging Interferometer are able to provide near-global coverage of the upper mesosphere for altitudes from 70 to 90 km. This study has shown that the temperature of this region can be successfully retrieved from Rayleigh-scattering sunlight measurements using the WINDII/UARS observations. A recent paper by *Shepherd et al.* [1999] has shown that the temperature field derived from WINDII can describe a number of wave-like structures such as quasi 2-day waves and tidal perturbations at the equatorial region. Since WINDII temperatures have been shown to correlate well with other established data sets, future dynamical studies may use a combination of WINDII daytime temperatures with the large database of nighttime temperature observations to provide a complete diurnal picture of the upper mesosphere. A long-term climatology of the mesosphere can also be developed from the SME measurements of the past decade and the WINDII/HRDI/MLS measurements of the current decade. An activity in the near future that would better facilitate the proposed work is to adapt the current retrieval algorithm to the WINDII level 2 data products with a very recent addition of level 2 background volume-scattering rates, which will greatly expand our mesospheric temperature database.

Acknowledgments. The WINDII project is sponsored by the Canadian Space Agency and the Centre National d'Etudes Spatial of France and supported by the Natural Science and Engineering Research Council of Canada. The authors thank Chiao Yao She for providing the CSU 1992 data. The research by one of our authors, B. Reid (Prawirosoehardjo) was supported by a graduate research grant of the Natural Science and Engineering Council of Canada. The derivation of the ALO temperatures at USU was supported by NSF CEDAR grant ATM9714789.

Janet G. Luhmann thanks both of the referees for their assistance in evaluating this paper.

References

Bills, R.E., and C.S. Gardner, Lidar observations of the mesopause region temperature structure at Urbana, *J. Geophys. Res., 98,* 1011-1021, 1993.

Bills, R.E., C.S. Gardner, and S.J. Franke, Na Doppler/temperature lidar: Initial mesopause region observations and comparison with the Urbana medium frequency radar, *J.Geophys. Res., 96,* 22,701-22,707, 1991.

Chahine, M., Inverse problems in radiative transfer: determination of atmospheric parameters, *J. Atmos. Sci., 27,* 960-967, 1970.

Chahine, M., A general relaxation method for inverse solution of the full radiative transfer equation, *J. Atmos. Sci., 29,* 741-747, 1972.

Chahine, M., Generalization of the relaxation method for the inverse solution of nonlinear and linear transfer equations, in *Inversion Methods in Atmospheric Remote Sounding*, Edited by A. Deepak, Academic, San Diego, Calif., 1977.

Chanin, M.L., and A. Hauchecorne, Lidar studies of the temperature and density using rayleigh scattering, *Handb. Middle Atmos. Progr., 13,* 87-99, 1984.

Chen, C., Z. Hu, M. White, D. Krueger, and C.Y. She, Lidar observations of seasonal variation of diurnal mean temperature in the mesopause region over Fort Collins, Colorado (41°N, 105°W), *J. Geophys. Res., 105,* 12,371-12,379, 2000.

Clancy, R.T., and D. Rusch, Climatology and trends of mesospheric (58-90 km) temperatures based upon 1982-1986 SME limb scattering profiles, *J. Geophys. Res., 94,* 3377-3393, 1989.

Clancy, R.T., D. Rusch, and M. Callan, Temperature minima in the average thermal structure of the middle mesosphere (70-80 km) from analysis of 40 to 92 km SME global temperature profiles, *J. Geophys Res., 99*, 19,001-19,020, 1994.

Dudhia, A., and N. Livesey, Validation of temperature measurements from the Improved Stratospheric and Mesospheric Sounder, *J. Geophys. Res., 101*, 9795-9810, 1996.

Evans, W. J., L. LaFramboise, and G. Shepherd, Mesospheric temperatures from Rayleigh scattering measurements by the WINDII instrument on UARS, *Adv. Space Res., 14*(9), 285-288, 1994.

Evans, W. F. J., L.R Laframboise, K.R. Sine, R.H. Wiens, and G.G. Shepherd, Observation of polar mesospheric clouds in summer, 1993 by the WINDII instrument on UARS, *Geophys. Res. Lett., 22*, 2793-2796, 1995.

Fishbein, E., et al., Validation of UARS Microwave Limb Sounder temperature and pressure measurements, *J. Geophys. Res., 101*, 9983-10,016, 1996.

Fleming, E., S. Chandra, M. Shoeberl, and J. Barnett, Monthly mean global climatology of temperature, wind, geopotential height, and pressure for 0-120 km, *NASA Tech. Memo. TM-100697*, 1988.

Gault, W.A., et al., Validation of O(^{1}S) wind measurements by WINDII: The WINDI imaging interferometer on UARS, *J. Geophys. Res., 101*, 10,405-10,430, 1996.

Hauchecorne, A., and M.L. Chanin, Density and temperature profiles obtained by lidar between 35 and 70 km, *Geophys. Res. Lett., 7*, 565-568, 1980.

Hauchecorne, A., M.L. Chanin, and R. Wilson, Mesospheric temperature inversion and gravity wave breaking, *Geophys. Res. Lett., 14*, 933-936, 1987.

Hauchecorne, A., M.L. Chanin, and P. Keckhut, Climatology and trends of the middle atmospheric temperatures (33-87 km) as seen by Rayleigh lidar over the south of France, *J. Geophys. Res., 96*, 15,297-15,309, 1991.

Hays, P.B., V.J. Abreu, M.E Dobbs, D.A. Gell, H.J. Grassl, and W.R. Skinner, The High-Resolution Doppler Imager on the Upper Atmosphere Research Satellite, *J. Geophys. Res., 96*, 1159-1172, 1993.

Hedin, A., Extension of the MSIS thermosphere model into the middle and lower atmosphere, *J. Geophys. Res., 96*, 1159-1172, 1991.

Leblanc, T., and A. Hauchecorne, Recent observations of mesospheric temperature inversions, *J. Geophys. Res., 102*, 19,471-19,482, 1997.

Lübken, F.J., The thermal structure of the Arctic summer mesopause, *J. Geophys Res., 104*, 9135-9149, 1999.

Lübken,, F.J., and U. von Zahn, Thermal structure of the mesopause region at polar latitudes, *J. Geophys. Res., 96*, 20,841-20,857, 1991.

Lübken,, F.J., K.H. Fricke, and M. Langer, Noctilucent clouds and the thermal structure near the Arctic mesopause in summer, *J. Geoph. Res., 101*, 9489-9508, 1996.

Meriwether, J., X. Gao, V. Wickwar, T. Wilkerson, K. Beissner, S. Collins, and M. Hagan, Observed coupling of the mesosphere inversion layer to the thermal tidal structure, *Geophys. Res. Lett., 25*, 1479-1482, 1998.

Ortland, D. A., P. B. Hayes and W. R. Skinner, Remote sensing of mesospheric temperature and $O_2(^1\Sigma)$ band volume emission rates with the high-resolution Doppler imager, *J. Geophys. Res., 103*, 1821-1835, 1998

Prawirosoehardjo, B., Retrieval and validation of mesospheric temperatures from WINDII observations, M.Sc. thesis, York Univ., Toronto, Ont., Canada, 1999.

Reber, C.A., C.E. Trevathan, R.J. McNeal, and M.R. Luther, The Upper Atmosphere Research Satellite (UARS) Mission, *J. Geophys Res., 98*, 10,643-10,647, 1993.

Rochon, Y., The retrieval of Doppler winds, temperatures, and emission rates for the WINDII experiment, Ph.D. thesis, York Univ., Toronto, Ont., Canada,1999.

Rogers, C.D., Retrieval of atmospheric temperature and composition from remote measurements of thermal radiations, *Rev. Geophys. Space Phys., 14*, 609-624, 1976.

Schmidlin, F., H. Lee, and W. Michel, The inflatable sphere: A technique for the accurate measurement of middle atmosphere temperatures, *J. Geophys. Res.*, 96, 22,673-22,682, 1991.

Senft, D.C., G.C. Papen, C.S. Gardner, J.R. Yu, D.A. Krueger, and C.Y. She, Seasonal variations of the thermal structure of the mesopause region at Urbana, IL (40°N, 88°W) and Ft. Collins, CO (41°N, 105°W), *Geophys. Res. Lett., 21*, 821-824, 1994.

She, C.Y., and U. von Zahn, Concept of a two-level mesopause: Support through new lidar observations, *J. Geophys. Res., 103*, 5855-5963, 1998.

She, C.Y., J.R. Yu, and H. Chen, Observed thermal structure of a midlatitude mesopause, *Geophys. Res. Lett., 20*, 567-570, 1993.

Shepherd, G., et al., WINDII, the Wind Imaging Interferometer on the Upper Atmosphere Research Satellite, *J. Geophys. Res., 98*, 10,725-10,750, 1993.

Shepherd, M., A. Dudhia, M. Lopez-Puertas, and W.F.J. Evans, Upper mesosphere temperatures in summer: WINDII observations and comparisons, *Geophys. Res. Lett., 24*, 357-360, 1997.

Shepherd, M., W. Ward, B. Prawirosoehardjo, R. Roble, S.-P. Zhang, and D. Wang, Planetary scale and tidal perturbations in mesospheric temperature observed by WINDII, *Earth Planets Space, 51*, 593-610, 1999.

Shepherd, M.G, P.J. Espy, C.Y. She, W. Hocking, P. Keckhut, G. Gavrilyeva, G.G. Shepherd, B. Naujokat, Springtime transition in upper mesospheric temperature in the Northern Hemisphere, *J. Atmos Sol. Terr. Phys.*, in press, 2001.

Singh, U., P. Keckhut, T.J. McGee, M.R. Gross, A. Houchecorne, E.F. Fishbein, J.W. Waters, J.C. Gille, A.E. Roche, and J.M. Russell III, Stratospheric temperature measurements by two collocated NDSC lidars during UARS validation campaign, *J. Geophys. Res., 101*, 10,287-10,297, 1996.

States, R.J., and C.S. Gardner, Influence of the diurnal tide and thermospheric heat sources on the formations of mesospheric temperature inversion layers, *Geophys. Res. Lett., 25*, 1483-1486, 1998.

States, R., and C. Gardner, Thermal structure of the mesopause region (80-105 km) at 40°N latitude. 1, Seasonal variations, *J. Atmos. Sci., 57*, 66-77, 2000a.

States, R., and C. Gardner, Thermal structure of the mesopause region (80-105 km) at 40°N latitude, 2 Diurnal Variations, *J. Atmos. Sci., 57*, 78-92, 2000b.

Taylor, F., et al., Remote sensing of atmospheric structure and composition by pressure modulator radiometry from space: The ISAMS experiment on UARS, *J. Geophys. Res., 98*, 10,799-10,814, 1993.

Thomas, G., Mesospheric clouds and the physics of the mesopause region, *Rev. Geophys., 29*, 553-575, 1991.

von Zahn, U., and W. Meyer, Mesopause temperatures in polar summer, *J. Geophys. Res., 94*, 14,647-14,651, 1989.

Whiteway, J., Lidar Observations of Atmospheric Gravity Wave Activity, Ph.D. thesis, York Univ., Toronto, Ont., Canada, 1994.

Wickwar, V.B., K.C. Beissner, T.D. Wilkerson, S.C. Collins, J.M. Maloney, J.W. Meriwether, Jr., and X. Gao, Climatology of mesospheric temperature profiles observed with the Consortium Rayleigh-scatter lidar at Logan, Utah, in *Advances in Atmospheric Remote Sensing with Lidar*, edited by A. Ansmann et al., pp. 557-560, Springer-Verlag, New York, 1997.

Wiens, R.H., S. Zhang, R.N. Peterson, and G.G. Shepherd, MORTI: A Mesopause Oxygen Rotational Temperature Imager, *Planet. Space Sci., 39*, 1363-1375, 1991.

Yu, J.R., and C.Y. She, Climatology of a midlatitude mesopause region observed by a lidar at Fort Collins, Colorado (40.6°N, 105°W), *J. Geophys. Res., 100*, 7441-7452, 1995.

Yu, J., R. States, S.J. Franke, C.S. Gardner, and M. Hagan, Observations of tidal temperature and wind perturbations in the mesopause region above Urbana, IL (40°N, 88°W), *Geophys. Res. Lett., 24*, 1207-1210, 1997.

J.P. Herron and V.B. Vickwar, Center for Atmospheric and Space Sciences, Utah State University, 4405 Old Main Hill, Logan, UT 84322-4405, USA; (herron@aeronomy.cass.usu.edu; wickwar@aeronomy.cass.usu.edu)

B. Reid, 4DM Inc, 4850 Keele St., Toronto, Ontario, Canada, M3J 3K1. (jreid@4dm-inc.com)

G.G. Shepherd, M.G. Shepherd, and B.H. Solheim, Centre for Research in Earth and Space Science, York University, 4700 Keele St., Toronto, Ontario, Canada M3J 1P3. (gordon@windii.yorku.ca; marianna@windii.yorku.ca; brian@windii.yorku.ca)

S. Zhang, MIT Haystack Observatory, Westford Route 40, Westford, MA 01886-1299. (szhang@haystack.mit.edu)

(Received August, 22, 2000; revised April 4, 2001;
accepted April 11, 2001.)